Roles of KLF4 and AMPK in the inhibition of glycolysis by pulsatile shear stress in endothelial cells

Yue Han[a,b], Ming He[b], Traci Marin[c], Hui Shen[b], Wei-Ting Wang[b], Tzong-Yi Lee[d], Hsiao-Chin Hong[d], Zong-Lai Jiang[a], Theodore Garland Jr[e], John Y.-J. Shyy[b,f,1], Brendan Gongol[b,c,1], and Shu Chien[f,g,1]

[a]Institute of Mechanobiology and Medical Engineering, School of Life Sciences & Biotechnology, Shanghai Jiao Tong University, Shanghai, 200240, China; [b]Department of Medicine, University of California San Diego, La Jolla, CA 92093; [c]Department of Health Sciences, Victor Valley College, Victorville, CA 92395; [d]Warshel Institute for Computational Biology, School of Life and Health Sciences, The Chinese University of Hong Kong, Shenzhen, 999077, China; [e]Department of Evolution, Ecology, and Organismal Biology, University of California, Riverside, CA 92521; [f]Institute of Engineering in Medicine, University of California San Diego, La Jolla, CA 92093; and [g]Department of Bioengineering, University of California San Diego, La Jolla, CA 92093

Contributed by Shu Chien, April 19, 2021 (sent for review March 4, 2021; reviewed by Y. Eugene Chen and Ying H. Shen)

Vascular endothelial cells (ECs) sense and respond to hemodynamic forces such as pulsatile shear stress (PS) and oscillatory shear stress (OS). Among the metabolic pathways, glycolysis is differentially regulated by atheroprone OS and atheroprotective PS. Studying the molecular mechanisms by which PS suppresses glycolytic flux at the epigenetic, transcriptomic, and kinomic levels, we have demonstrated that glucokinase regulatory protein (GCKR) was markedly induced by PS in vitro and in vivo, although PS down-regulates other glycolysis enzymes such as hexokinase (HK1). Using next-generation sequencing data, we identified the binding of PS-induced Krüppel-like factor 4 (KLF4), which functions as a pioneer transcription factor, binding to the GCKR promoter to change the chromatin structure for transactivation of GCKR. At the posttranslational level, PS-activated AMP-activated protein kinase (AMPK) phosphorylates GCKR at Ser-481, thereby enhancing the interaction between GCKR and HK1 in ECs. In vivo, the level of phosphorylated GCKR Ser-481 and the interaction between GCKR and HK1 were increased in the thoracic aorta of wild-type AMPKα2$^{+/+}$ mice in comparison with littermates with EC ablation of AMPKα2 (AMPKα2$^{-/-}$). In addition, the level of GCKR was elevated in the aortas of mice with a high level of voluntary wheel running. The underlying mechanisms for the PS induction of GCKR involve regulation at the epigenetic level by KLF4 and at the posttranslational level by AMPK.

AMPK | KLF4 | epigenetics | GCKR | glycolysis

The endothelium lines the luminal surface of the arterial wall and is in direct contact with blood flow. The pulsatile shear stress (PS) at straight parts of arteries maintains endothelial homeostasis, whereas oscillatory shear stress (OS) at bifurcations and curvatures impairs endothelial function. Such OS-induced endothelial cell (EC) dysfunction is characterized by enhanced glycolysis, inflammation, proliferation, and production of reactive oxygen species (ROS) (1–5). Collectively, these EC phenotypic changes cause atherosclerosis (6).

As the sole pathway for glucose catabolism, glycolysis is a main energy source for the endothelium (7–9). Increased glycolysis in ECs meets the demand of glucose consumption required for EC migration and proliferation (3, 10). However, exaggerated glycolysis in endothelium is associated with disease states such as tumor angiogenesis, diabetic retinopathy, and atherosclerosis (8, 9). Mounting evidence indicates that shear stress regulates glycolysis in ECs as a function of the flow patterns. Doddaballapur et al. showed that the PS-induced Krüppel-like factor 2 (KLF2) reduces metabolic activity in ECs by repressing the expression of 6-phosphofructo-2-kinase/fructose-2,6-biphosphatase 3 (PFKFB3), a key regulator of glycolysis (1). Analyzing RNA-sequencing (RNA-seq) data from ECs exposed to OS, Wu et al. concluded that OS increases endothelial glycolysis via stabilization of ROS-mediated hypoxia-inducible factor 1α (HIF-1α) (11). Using bulk assays, Feng et al. reported a similar result, namely, OS increased EC proliferation and inflammation via HIF-1α induction of glycolysis enzymes (12). While these reports pointed out the increase in glycolysis under OS, a systemic study of the regulatory mechanisms of glycolysis in the endothelium in response to distinct flow patterns remains elusive.

Krüppel-like factor 4 (KLF4) and AMP-activated protein kinase (AMPK) are two principal molecules involved in the mechanotransduction mechanism in ECs. KLF4 is one of the Yamanaka factors that are necessary for embryonic cell pluripotency (13, 14). In ECs, KLF4 is a lineage-dependent transcription factor (TF) essential for endothelial lineage and a PS-induced signal-dependent TF (14). Under PS, KLF4 transcriptionally up-regulates many atheroprotective genes such as endothelial nitric oxide synthase (eNOS), thrombomodulin, and inositol 1,4,5-trisphosphate receptor, type 3 (ITPR3) (15, 16). Functioning as a pioneer TF, KLF4 binds to the promoter region of these PS-induced genes to interact with the basal transcriptional machinery and initiate epigenetic remodeling (16). As a metabolic gauge, AMPK globally regulates cellular metabolism by increasing catabolic pathways and decreasing anabolic pathways. AMPK activation decreases energy-consuming glycolysis while promoting mitochondrial oxidative metabolism to restore energy homeostasis (17). Upon activation, AMPK phosphorylates a number of target proteins in ECs that

Significance

This work identifies mechanotransduction mechanisms by which blood flow regulates glycolysis in vascular endothelium. We demonstrate that atheroprotective flow pattern decreases glycolysis, an energy-demanding metabolic process, in endothelium in vitro and in vivo. GCKR, an inhibitor of glycolytic flux, is up-regulated by atheroprotective flow, in contrast to the down-regulation of other glycolysis genes. As a pioneer transcription factor induced by atheroprotective flow, KLF4 epigenetically remodels the GCKR promoter and thus transactivates GCKR. At the posttranslational level, atheroprotective flow–activated AMPK phosphorylates GCKR and hence increases GCKR binding to hexokinase, the key enzyme in glycolysis. The translational significance of these findings builds on the identification of these atheroprotective mechanisms in an animal model with a high level of voluntary wheel running.

Author contributions: T.G., J.Y.-J.S., B.G., and S.C. designed research; Y.H., M.H., T.M., H.S., W.-T.W., T.-Y.L., H.-C.H., Z.-L.J., and B.G. performed research; Y.H. and B.G. analyzed data; and J.Y.-J.S., B.G., and S.C. wrote the paper.

Reviewers: Y.E.C., University of Michigan Medical School; and Y.H.S., Baylor College of Medicine.

The authors declare no competing interest.

[1]To whom correspondence may be addressed. Email: jshyy@ucsd.edu, brendan.gongol@ucr.edu, or shuchien@ucsd.edu.

This article contains supporting information online at https://www.pnas.org/lookup/suppl/doi:10.1073/pnas.2103982118/-/DCSupplemental.

Published May 17, 2021.

contain a βθβXXX(S/T)XXXθ consensus sequence (β = basic amino acid, θ = hydrophobic amino acid, and X = any amino acid) (18). Many of these AMPK substrate proteins, such as eNOS and angiotensin converting enzyme 2, are critical for endothelial homeostasis (19, 20).

Hexokinase (HK1) catalyzes the first and also rate-limiting step of glycolysis. HK IV, also called glucokinase (GK), is expressed abundantly in ECs. Glycolysis is inhibited by the binding of glucokinase regulator protein (GCKR) to HK1, thereby sequestering HK1 in the nucleus (21). In homeostatic state, GCKR is usually present in molar excess of HK1 in the cell. However, the glycolytic rate is affected by the level of GCKR and the binding status of GCKR/HK1, which is dynamically and intricately modulated and can be rapidly changed by metabolic conditions (22). Thus, the expression of GCKR and its posttranslational modifications are essential regulatory mechanisms in glycolysis (23).

Given the lack of information on how shear stress regulates EC glycolysis via GCKR, we launched this study to investigate the roles of KLF4 and AMPK in regulating EC glycolysis via GCKR. Our results show that PS down-regulates glycolysis in ECs by 1) KLF4-mediated epigenetic and transcriptional up-regulation of GCKR expression and 2) AMPK phosphorylation of GCKR, with the ensuing increase in GCKR/HK1 interaction. This mechanotransduction mechanism is recapitulated in vascular health in mice with a high level of voluntary wheel running behavior.

Results

PS Down-Regulates Glycolysis in ECs at the Systems Level. We first assessed the dynamic changes in expression of genes involved in the glycolysis pathway in response to PS vs. OS by analyzing RNA-seq data from human umbilical vein ECs (HUVECs) subjected to PS and OS for 0 to 24 h (GSE103672) (16, 24). Pathway analysis demonstrated that the enzymes involved in glycolytic steps were generally down-regulated by PS starting from 16 h, as compared with OS (Fig. 1*A*). These results confirm that PS and OS regulate glycolysis in ECs in opposite directions. The RNA-seq findings that PS suppressed glycolysis enzymes were validated by qPCR (Fig. 1*B*). Because epigenetic regulations are integral parts of mechanotransduction in ECs in response to shear stress (16), we next investigated whether PS down-regulation of glycolysis genes involves chromatin remodeling. Thus, we determined the enrichment of transposase-accessible chromatin sequencing (ATAC-seq) peaks (measuring decondensed chromatin structure) in the regions flanking the transcription start site of the human glycolysis gene. The promoter regions of these glycolysis genes exhibited ATAC peak enrichment under OS vs. PS (Fig. 1*C*). Together, these results indicate that the PS inhibition of glycolysis genes occurs at epigenetic and transcriptional levels.

KLF4 Regulates GCKR Expression in Response to PS. In addition to testing PS down-regulated genes, we also examined PS up-regulated genes involved in glycolysis. PS markedly induced GCKR transcripts during 24 h (Fig. 2*A*), and this was validated by qPCR (Fig. 2*B*). We next examined the effect of PS on H3K27ac enrichment in the promoter region of GCKR. PS enriched H3K27ac signals (Fig. 2*C*), indicating that the GCKR promoter has a more decondensed chromatin structure under PS than OS. Given that KLF4 is a PS-induced pioneer TF transactivating a panel of genes essential for EC homeostasis (16), we next explored whether the PS-induced GCKR is mediated by KLF4 epigenetically and transcriptionally. Among the putative TFs that can bind to the GCKR promoter (determined by analyzing the binding sites for transcription factors [BSTF]), KLF4 mRNA was induced to the greatest extent by PS, according to the GSE103672 dataset (Fig. 2*D*). Consistent with the two putative KLF4 binding sites predicted in the GCKR promoter (Fig. 2*C*), GCKR was induced in ECs overexpressing KLF4, as indicated by the RNA-seq data (GSE90982, Fig. 2*E*). To validate the results in Fig. 2 *A*–*E*, we

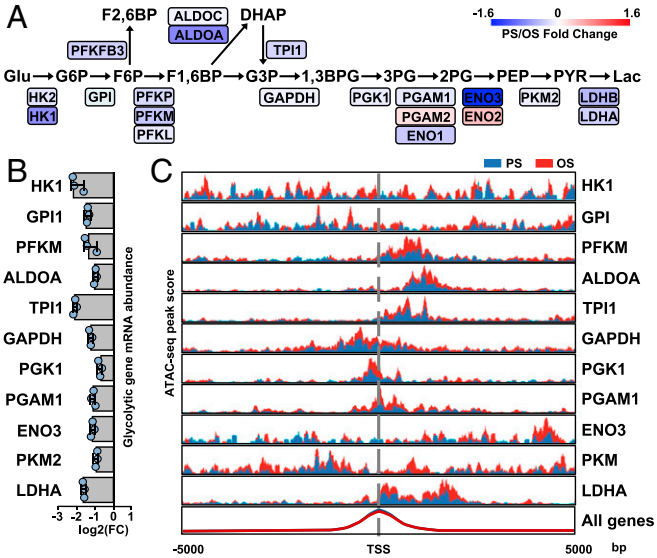

Fig. 1. PS inhibits the expression of glycolysis genes in ECs. (*A*) Pathway diagram generated from RNA-seq data (GSE103672) analyzing HUVECs exposed to PS (12 ± 4 dyn/cm^2) or OS (1 ± 4 dyn/cm^2) for 0 to 24 h. The PS/OS fold changes of the mRNAs are shown with colors indicated in the scale on the *Upper Right*. Data are represented as the average fold changes at 12-, 16-, and 24-h time points. (*B*) Relative PS/OS mRNA levels of indicated glycolytic genes (detected by qPCR) in HUVECs exposed to PS or OS for 16 h. (*C*) ATAC-seq analysis of HUVECs exposed to PS or OS for 16 h in three biological repeats. The promoter regions of the glycolysis genes exhibited ATAC peak enrichment under PS (area in blue) or OS (area in red). Data are mean ± SEM from three independent experiments.

overexpressed KLF4 in ECs, mimicking the PS induction of KLF4. KLF4 overexpression increased KLF4 binding to the GCKR promoter and the expression of GCKR, as assessed by KLF4 chromatin immunoprecipitation (ChIP)-PCR, qPCR, and Western blot (Fig. 2 *F*–*H*). In reciprocal experiments with KLF4 knockdown in ECs, the PS induction of GCKR was attenuated at both mRNA and protein levels (Fig. 2 *I* and *J*). In line with these results, PS increased KLF4 binding to the GCKR promoter and augmented GCKR expression (Fig. 2 *B*, *K*, and *L*). The mouse thoracic aorta (TA) and aortic arch (AA) are under atheroprotective vs. atheroprone flow patterns. In vivo validation was provided by the finding that the GCKR mRNA level was higher in intima isolated from TA than AA (Fig. 2*M*). Taken together, the results in Fig. 2 demonstrate that the PS-induced GCKR depends on KLF4-mediated epigenetic and transcriptional regulations.

AMPK Phosphorylates and Regulates GCKR. The activities of several glycolysis enzymes (e.g., Phosphofructokinase 1 [PFK1]) are regulated by posttranslational modifications such as phosphorylation. To determine whether the PS-induced GCKR also involves protein phosphorylation, we used bioinformatics approaches to determine the phosphorylation sites and the corresponding kinases that phosphorylate GCKR. To accomplish this, kinase phosphorylation sites of GCKR were predicted first by evaluating the conservation of these sites among species using the Ensembl database (25). Then, kinases that putatively phosphorylate GCKR were ranked, based on the conservation of the cognate phosphorylation site. Among the predicted kinases, AMPK had the most preserved consensus sequences (Fig. 3*A*). To test whether AMPK can directly phosphorylate GCKR, we used in vitro kinase assays. Kinase reaction mixture containing recombinant AMPK caused an increase of the phosphorylation of GCKR (Fig. 3*B*). Among the seven putative AMPK phosphorylation sites, Ser-481 was the most homologous to the AMPK phosphorylation consensus sequence

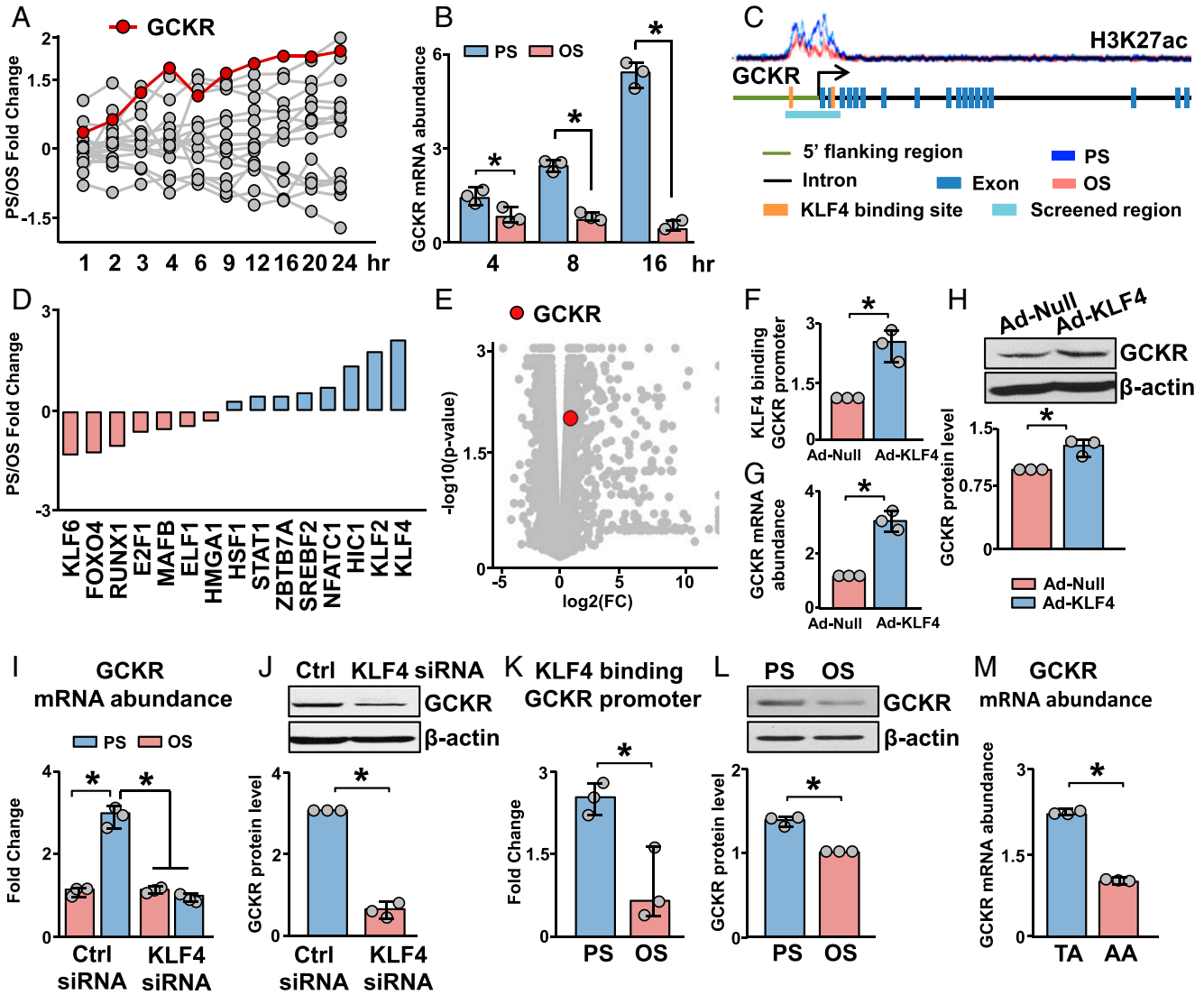

Fig. 2. KLF4 regulates the expression of GCKR in response to PS. (*A*) Time course of PS/OS fold changes in mRNA level with a "glycolysis" gene ontology categorization in ECs exposed to PS or OS for 24 h. (*B*) qPCR analysis of GCKR mRNA expression in HUVECs subjected to PS or OS at 4, 8, and 16 h. (*C*) Level of H3K27ac in the GCKR promoter, which is annotated with the regions screened for TF binding sites. (*D*) RNA-seq data showing PS/OS fold change of TFs identified in the GCKR promoter as illustrated in *C*. (*E*) GCKR fold change and significance in RNA-seq data from HUVECs infected with Ad-null or Ad-KLF4 for 48 h. (*F–H*) HUVECs were infected with Ad-KLF4 for 48 h. Level of KLF4 binding to the GCKR promoter is shown in *F*, GCKR mRNA abundance in *G*, and GCKR protein abundance in *H*. (*I*) Levels of GCKR mRNA in HUVECs transfected with control (Ctrl) siRNA or KLF4 siRNA and subjected to PS or OS, respectively. (*J*) Levels of GCKR protein in HUVECs transfected with Ctrl siRNA or KLF4 siRNA and subjected to PS. (*K* and *L*) HUVECs were subjected to PS or OS. KLF4 binding to the GCKR promoter is shown in *K* and GCKR protein abundance in *L*. (*M*) GCKR mRNA abundance in the TA and AA from 7-wk-old C57BL/6 mice. $*P < 0.05$. Data are mean ± SEM from three independent experiments.

(*SI Appendix*, Fig. S1 *A* and *B*). To test whether GCKR Ser-481 was indeed an AMPK phosphorylation site, we mutated Ser-481 to Ala (S481A), and then conducted in vitro kinase assays using the wild-type and S481A mutant proteins. AMPK phosphorylation of GCKR S481A was attenuated as compared with the wild-type GCKR (Fig. 3*B*). In comparison to OS, PS increased the phosphorylation of GCKR Ser-481 in mouse embryonic fibroblasts (MEFs) (Fig. 3*C*). Also, AMPK-knockout ($AMPK^{-/-}$) MEFs showed little phosphorylation of GCKR Ser-481 (Fig. 3*C*). Next, we tested whether the phosphorylation of GCKR Ser-481 by AMPK regulates the GCKR–HK1 interaction that inhibits glycolysis (23, 26, 27). As anticipated, PS-induced GCKR–HK1 interaction was attenuated in HUVECs transfected with GCKR S481A (dephosphomimetic) and was sustained in HUVECs transfected with GCKR S481D (phosphomimetic) (Fig. 3*D*). Functionally, HK1 activity was higher in HUVECs expressing GCKR S481A than those expressing S481D (Fig. 3*E*). In vivo studies showed that GCKR Ser-481 phosphorylation and GCKR–HK1 interaction were higher in the TA from $AMPK\alpha2^{+/+}$ than $AMPK\alpha2^{-/-}$ mice (Fig. 3 *F* and *G*). Overall, the results in Fig. 3 indicate that PS increased AMPK phosphorylation of GCKR Ser-481, which in turn enhanced GCKR–HK1 interaction to attenuate HK1 activity in ECs.

KLF4-AMPK/GCKR Inhibition of Glycolysis in Mice with a High Level of Voluntary Running. We used adult males from a selectively bred mouse model (generation 83) with a high level of voluntary wheel running, namely, high-runner (HR) mice (28), to substantiate the finding that KLF4-AMPK/GCKR inhibits glycolysis in the endothelium in vivo. Presumably, PS is increased in the aorta of these HR mice as a result of the increase in cardiac output (29), and we

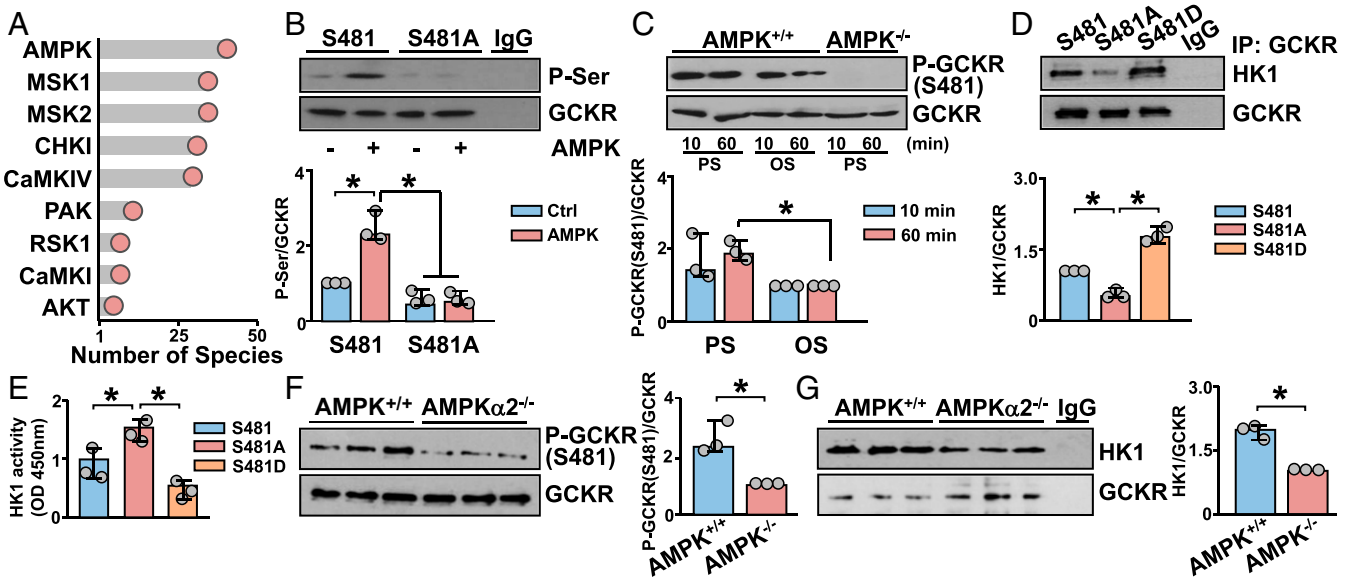

Fig. 3. AMPK phosphorylates and regulates GCKR. (*A*) Number of species that contain GCKR phosphorylation sites phosphorylated by various kinases as indicated. (*B*) In vitro kinase assays with immunopurified GCKR or GCKR S481A (dephosphomimetic) with or without recombinant AMPK. (*C*) Compared with OS, PS increased the phosphorylation of GCKR S481 in AMPK$^{+/+}$ MEFs at 10 and 60 min. In contrast, AMPK$^{-/-}$ MEFs showed little phosphorylation of GCKR S481. (*D* and *E*) HUVECs were transfected with GCKR S481, S481A, or S481D (phosphomimetic) expression plasmids for 2 d. GCKR coimmunoprecipitated with HK1 is shown in *D* and HK1 activity in *E*. (*F* and *G*) Aortic tissues were isolated from the TA parts of AMPKα2$^{+/+}$ and AMPKα2$^{-/-}$ mice. Level of GCKR Ser-481 phosphorylation is shown in *F* and interaction with HK1 in *G*. *$P < 0.05$. Data are mean ± SEM from three independent experiments.

previously showed that AMPK activity is increased in aortas from these mice (29). With such background information, we tested whether glycolysis is decreased in the aorta of HR mice (sampled from HR line #7) as compared with nonselected control mice (C) (sampled from C line #4) sedentary mice. Both HR and C mice had access to wheels (28) for 4 wk prior to killing.

qPCR revealed lower expression of glycolysis genes in HR than C mice (Fig. 4*A*). KLF4 binding to the GCKR promoter was enhanced and GCKR mRNA level was higher in the aortas of HR than C mice (Fig. 4 *B* and *C*), consistent with the notion that PS induces GCKR via KLF4. The protein levels of KLF4 and GCKR were also higher in HR than C aortas (Fig. 4*D*). In line with the observation that PS modulates GCKR activity via AMPK, the phosphorylation of GCKR Ser-481 and the GCKR–HK1 interaction were enhanced in HR vs. C mice (Fig. 4 *E* and *F*). Moreover, HK1 activity was decreased in aortas of HR vs. C mice (Fig. 4*G*). Overall, the data in Fig. 4 suggest that aerobic exercise may benefit vascular endothelium in energy utilization, and that this beneficial outcome is mediated by increased GCKR expression and activity. The underpinning mechanisms should include regulations by KLF4 and AMPK at the transcriptional and post-translational levels, respectively (Fig. 5).

Discussion

This study demonstrates a mechanism by which PS attenuates glycolysis via suppressing GCKR, which is coordinately regulated at epigenetic, transcriptomic, and proteomic levels, as based on two key findings. First, the PS-induced KLF4 increased the expression of GCKR, but suppressed that of glycolytic genes. The suppression of HK1 together with GCKR induction led to an increased molar ratio of GCKR to HK1. Second, the PS-induced AMPK phosphorylated GCKR Ser-481, thus increasing the GCKR–HK1 interaction. The augmented GCKR-to-HK1 ratio and GCKR–HK1 interaction would restrict the first and key step of glycolysis, namely, the conversion of glucose to glucose 6-phosphate in ECs under atheroprotective flow (Fig. 5). Given that glycolysis is an essential pathway for the utilization of glucose to support EC metabolism, this mechanism newly defined in the present study may act in concert with other fine-tuned metabolic pathways to maintain a functional endothelium.

We and others have previously shown that epigenetics (pioneer TFs, DNA methylation, and histone modifications) are integral to the shear stress regulation of gene expression and EC phenotypes (16, 17). Pioneer TFs bind to *cis*-regulatory elements and recruit DNA methyltransferases, histone acetyltransferases, or histone deacetylases to coordinate DNA methylation and histone modifications for transcriptional regulation (30, 31). There is ample evidence that the PS-induced KLF4 acts as a pioneer TF to transactivate a plethora of genes (e.g., eNOS, tropomodulin, ITPR3, etc.) in ECs. Several lines of evidence support that KLF4-coordinated epigenetic regulations are essential for the PS induction of these genes: 1) KLF4, as an EC lineage-dependent TF, is able to bind to the promoter regions of KLF4 target genes; 2) PS stimulation induces an open state of these promoter regions encompassing or flanking KLF4 binding sites; and 3) KLF4 overexpression in ECs recapitulates the PS-driven chromatin remodeling and transactivation. The present study shows that the KLF4-induced GCKR (Fig. 2 *E–J*) is mediated through these mechanisms. In parallel to KLF4, KLF2 is another robust pioneer TF enabling the transcriptional activation of these beneficial genes in response to PS. Whether KLF2 orchestrates similar epigenetic regulations as KLF4 to induce GCKR warrants future studies.

ECs produce as much as 85% of ATP from glycolysis rather than oxidative phosphorylation. When under angiogenic, turnover, or stress conditions, ECs become even more glycolytic to meet the energy demand. We previously showed that PS or metformin activates AMPK to enhance mitochondrial abundance and function, resulting in elevated ATP level and reduced mitochondrial-derived ROS in ECs (17). In the current study, we showed that AMPK phosphorylates GCKR, with ensuing formation of the GCKR–HK1 complex. Thus, the PS-activated AMPK maintains EC energy homeostasis by enhanced mitochondrial efficiency and reduced glycolytic flux. Although previous reports indicated that AMPK inhibits glycolysis by phosphorylating GCKR in hepatocytes (23, 26, 27), our results in Fig. 3 reveal GCKR Ser-481 as a key site phosphorylated by AMPK in response to PS. These results

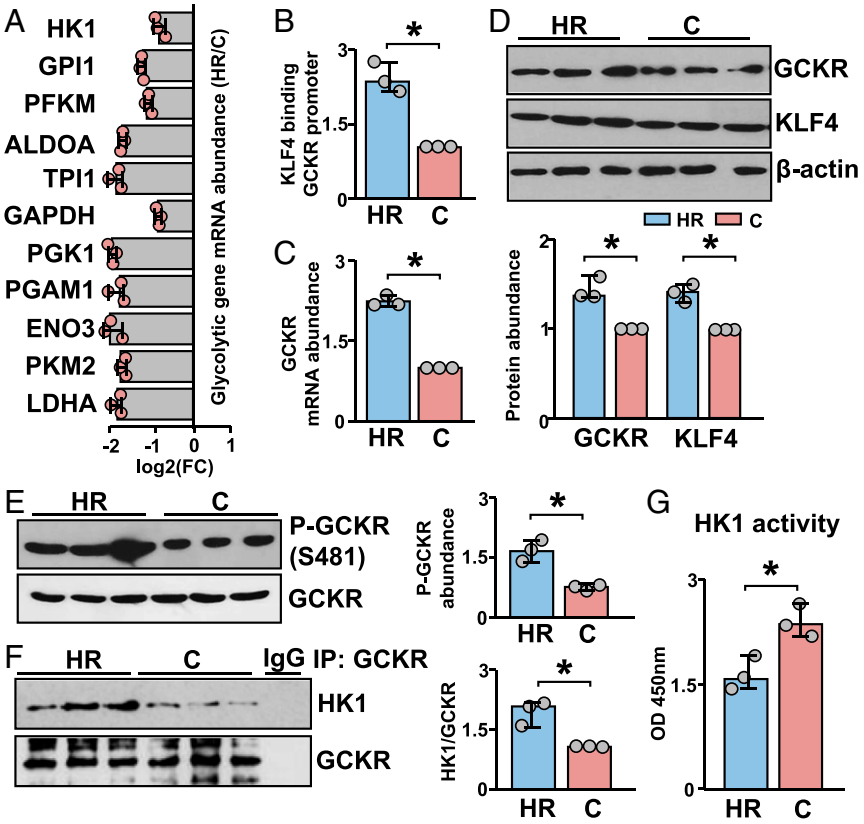

Fig. 4. KLF4-AMPK/GCKR inhibition of glycolysis in mice with high level of voluntary wheel running. TAs were isolated and pooled from 7-wk-old mice with high level of voluntary wheel running (HR, three male) and nonselected control-line mice (C, three male), all of which had wheel access for 4 wk. (*A*) qPCR analysis of mRNA levels of glycolysis genes in the isolated TAs. (*B*) KLF4 binding to the GCKR promoter, detected by ChIP-PCR. (*C*) qPCR analysis of GCKR mRNA level. (*D* and *E*) Western blots of GCKR, KLF4 and phosphorylated GCKR Ser-481 and GCKR. (*F*) GCKR coimmunoprecipitated with HK1. (*G*) HK1 activity. Data are mean ± SEM from three mice. $*P < 0.05$.

are strengthened by the in vivo findings that phosphorylation of S481 GCKR was impaired in the aortas of AMPKα2$^{-/-}$ mice and that this impairment was accompanied by the enhanced HK1 activity. Because both AMPKα2$^{-/-}$ and GCKR$^{-/-}$ mice exhibit impaired glucose metabolism (32, 33), AMPK phosphorylation of GCKR Ser-481 may be functional in issue types other than endothelium, such as liver or skeletal muscle, which deserves future study. Additionally, the Ser-481 phosphorylation of GCKR may synergize with other posttranslational modifications of GCKR, including the acetylation or ubiquitination of Lys-5 (34). One intriguing question is whether Ser-481 phosphorylation affects the structure of the HK binding domain and therefore facilitates GCKR-HK1 binding. As such, we performed an analysis on the location of S481 in relation to the HK binding domain on GCKR. As shown in *SI Appendix*, Fig. S3, the GCKR-HK binding occurs via a β-sheet structure on GCKR that results in multiple noncovalent interactions with HK. Apparently, S481 is located adjacent to the β-sheet. Although our results indicate that AMPKα2 is activated by PS to inhibit glycolysis, the regulation of AMPK in the vasculature may depend on the specific AMPK isoform and the time durations of activation (35).

The temporal dynamics of epigenetic, transcriptional, and posttranslational regulations are synergistically involved in the transactivation of metabolically related genes. We found that AMPK phosphorylation of GCKR occurred within 10 min after the onset of PS. However, the transcriptional induction of GCKR did not reach a steady state until 12 h after PS onset (Fig. 2*A* and *B*). Blood flow varies dynamically in the arterial tree; the spatiotemporal regulation of GCKR in the vascular endothelium in vivo is tightly controlled at the systems level. A comprehensive and coordinated regulation of GCKR is indispensable for regulating the energy status in the endothelium in the context of glycolysis.

The clinical relationship between enhanced glycolysis and vascular disease is well established. At the cellular level, increased glycolytic activity leads to enhanced oxidative stress, inflammation, and endothelial cell proliferation, all associated with EC dysfunction and the onset of many cardiovascular diseases (1–5, 10, 36, 37). To this end, voluntary wheel running of mice would maintain AMPK at a more activated state within the vascular tree and hence improve EC function (28). Metabolically, this beneficial effect is mediated at least in part by the synergistic regulation of GCKR by KLF4 and AMPK, leading to attenuated glycolysis (Fig. 5).

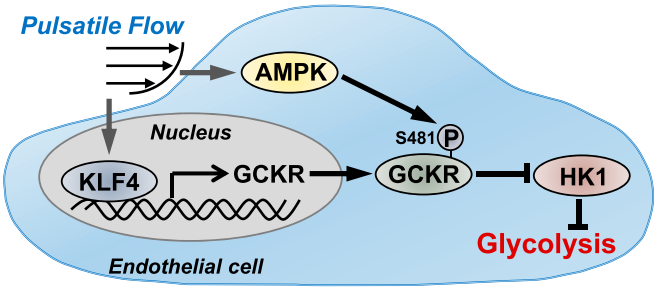

Fig. 5. Summary diagram of PS inhibition of glycolysis in ECs via KLF4 and AMPK.

Ultimately, such reduction in EC glycolysis by physiological activities may be important for the maintenance of vascular health.

Materials and Methods

Experimental methods are described in detail in *SI Appendix, SI Materials and Methods*. Cells for all experiments were cultured according to standard procedures and kept in a standard cell culture incubator held at 37 °C and 5% CO_2. Quantification of nucleic acids by qPCR was conducted with a Bio-Rad CFX96 real-time detection system using SYBR green. All primers used for ChIP or standard PCR are listed in *SI Appendix*, Table S1. Bioinformatic analyses were conducted in R programming language with support from Bioconductor or Comprehensive R Archive Network (CRAN) libraries.

Data Availability. All study data are included in the article and/or *SI Appendix*.

ACKNOWLEDGMENTS. This work was supported by NIH Grants R01HL108735 and R01HL106579 (to S.C. and J.Y.-J.S.) and 5T32HL134632-02 (to B.G.) and by the National Natural Science Foundation of China Grant (No. 12072197) (to Y.H.). T.G. was supported by NSF Grant DEB-1655362. We acknowledge Drs. Jian Kang, Jiao Zhang, and Marcy Martin for their technical assistance.

1. A. Doddaballapur *et al*., Laminar shear stress inhibits endothelial cell metabolism via KLF2-mediated repression of PFKFB3. *Arterioscler. Thromb. Vasc. Biol.* **35**, 137–145 (2015).
2. J. Wang, S. Zhang, Fluid shear stress modulates endothelial inflammation by targeting LIMS2. *Exp. Biol. Med. (Maywood)* **245**, 1656–1663 (2020).
3. S. Chien, Effects of disturbed flow on endothelial cells. *Ann. Biomed. Eng.* **36**, 554–562 (2008).
4. K. S. Heo, K. Fujiwara, J. Abe, Disturbed-flow-mediated vascular reactive oxygen species induce endothelial dysfunction. *Circ. J.* **75**, 2722–2730 (2011).
5. P. F. Davies, A. Remuzzi, E. J. Gordon, C. F. Dewey, Jr, M. A. Gimbrone, Jr, Turbulent fluid shear stress induces vascular endothelial cell turnover in vitro. *Proc. Natl. Acad. Sci. U.S.A.* **83**, 2114–2117 (1986).
6. J. J. Chiu, S. Chien, Effects of disturbed flow on vascular endothelium: Pathophysiological basis and clinical perspectives. *Physiol. Rev.* **91**, 327–387 (2011).
7. K. Theodorou, R. A. Boon, Endothelial cell metabolism in atherosclerosis. *Front. Cell Dev. Biol.* **6**, 82 (2018).
8. K. Rohlenova, K. Veys, I. Miranda-Santos, K. De Bock, P. Carmeliet, Endothelial cell metabolism in health and disease. *Trends Cell Biol.* **28**, 224–236 (2018).
9. G. Eelen, P. de Zeeuw, M. Simons, P. Carmeliet, Endothelial cell metabolism in normal and diseased vasculature. *Circ. Res.* **116**, 1231–1244 (2015).
10. K. De Bock, M. Georgiadou, P. Carmeliet, Role of endothelial cell metabolism in vessel sprouting. *Cell Metab.* **18**, 634–647 (2013).
11. D. Wu *et al*., *HIF-1α* is required for disturbed flow-induced metabolic reprogramming in human and porcine vascular endothelium. *eLife* **6**, e25217 (2017).
12. S. Feng *et al*., Mechanical activation of hypoxia-inducible factor 1α drives endothelial dysfunction at atheroprone sites. *Arterioscler. Thromb. Vasc. Biol.* **37**, 2087–2101 (2017).
13. A. Young *et al*., Flow activation of AMP-activated protein kinase in vascular endothelium leads to Krüppel-like factor 2 expression. *Arterioscler. Thromb. Vasc. Biol.* **29**, 1902–1908 (2009). Corrected in: *Arterioscler. Thromb. Vasc. Biol.* **30**, e325 (2010).
14. Y. Fan *et al*., Krüppel-like factors and vascular wall homeostasis. *J. Mol. Cell Biol.* **9**, 352–363 (2017).
15. G. Zhou *et al*., Endothelial Kruppel-like factor 4 protects against atherothrombosis in mice. *J. Clin. Invest.* **122**, 4727–4731 (2012).
16. M. He *et al*., Atheroprotective flow upregulates ITPR3 (Inositol 1,4,5-Trisphosphate Receptor 3) in vascular endothelium via KLF4 (Krüppel-Like Factor 4)-mediated histone modifications. *Arterioscler. Thromb. Vasc. Biol.* **39**, 902–914 (2019).
17. T. L. Marin *et al*., AMPK promotes mitochondrial biogenesis and function by phosphorylating the epigenetic factors DNMT1, RBBP7, and HAT1. *Sci. Signal.* **10**, eaaf7478 (2017).
18. T. L. Marin *et al*., Identification of AMP-activated protein kinase targets by a consensus sequence search of the proteome. *BMC Syst. Biol.* **9**, 13 (2015).
19. B. Thors, H. Halldórsson, G. Thorgeirsson, eNOS activation mediated by AMPK after stimulation of endothelial cells with histamine or thrombin is dependent on LKB1. *Biochim. Biophys. Acta* **1813**, 322–331 (2011).
20. J. Zhang *et al*., AMP-activated protein kinase phosphorylation of angiotensin-converting enzyme 2 in endothelium mitigates pulmonary hypertension. *Am. J. Respir. Crit. Care Med.* **198**, 509–520 (2018).
21. A. Raimondo, M. G. Rees, A. L. Gloyn, Glucokinase regulatory protein: Complexity at the crossroads of triglyceride and glucose metabolism. *Curr. Opin. Lipidol.* **26**, 88–95 (2015).
22. M. Salgado *et al*., When a little bit more makes the difference: Expression levels of GKRP determines the subcellular localization of GK in tanycytes. *Front. Neurosci.* **13**, 275 (2019).
23. B. Guigas *et al*., 5-Aminoimidazole-4-carboxamide-1-beta-D-ribofuranoside and metformin inhibit hepatic glucose phosphorylation by an AMP-activated protein kinase-independent effect on glucokinase translocation. *Diabetes* **55**, 865–874 (2006).
24. N. E. Ajami *et al*., Systems biology analysis of longitudinal functional response of endothelial cells to shear stress. *Proc. Natl. Acad. Sci. U.S.A.* **114**, 10990–10995 (2017).
25. D. R. Zerbino *et al*., Ensembl 2018. *Nucleic Acids Res.* **46**, D754–D761 (2018).
26. L. Agius, Hormonal and metabolite regulation of hepatic glucokinase. *Annu. Rev. Nutr.* **36**, 389–415 (2016).
27. A. Šmerc, E. Sodja, M. Legiša, Posttranslational modification of 6-phosphofructo-1-kinase as an important feature of cancer metabolism. *PLoS One* **6**, e19645 (2011).
28. Y. Zhang *et al*., AMP-activated protein kinase is involved in endothelial NO synthase activation in response to shear stress. *Arterioscler. Thromb. Vasc. Biol.* **26**, 1281–1287 (2006).
29. L. M. Vaanholt *et al*., Metabolic and behavioral responses to high-fat feeding in mice selectively bred for high wheel-running activity. *Int. J. Obes.* **32**, 1566–1575 (2008).
30. K. S. Zaret, Pioneer transcription factors initiating gene network changes. *Annu. Rev. Genet.* **54**, 367–385 (2020).
31. A. Moosavi, A. Motevalizadeh Ardekani, Role of epigenetics in biology and human diseases. *Iran. Biomed. J.* **20**, 246–258 (2016).
32. J. Grimsby *et al*., Characterization of glucokinase regulatory protein-deficient mice. *J. Biol. Chem.* **275**, 7826–7831 (2000).
33. B. Viollet *et al*., Physiological role of AMP-activated protein kinase (AMPK): Insights from knockout mouse models. *Biochem. Soc. Trans.* **31**, 216–219 (2003).
34. J. M. Park, T. H. Kim, S. H. Jo, M. Y. Kim, Y. H. Ahn, Acetylation of glucokinase regulatory protein decreases glucose metabolism by suppressing glucokinase activity. *Sci. Rep.* **5**, 17395 (2015).
35. Q. Yang *et al*., PRKAA1/AMPKα1-driven glycolysis in endothelial cells exposed to disturbed flow protects against atherosclerosis. *Nat. Commun.* **9**, 4667 (2018).
36. G. Soto-Heredero, M. M. Gómez de Las Heras, E. Gabandé-Rodríguez, J. Oller, M. Mittelbrunn, Glycolysis–A key player in the inflammatory response. *FEBS J.* **287**, 3350–3369 (2020).
37. C. M. Grant, Metabolic reconfiguration is a regulated response to oxidative stress. *J. Biol.* **7**, 1 (2008).

PNAS
www.pnas.org

Supplementary Information for

Roles of KLF4 and AMPK in the Inhibition of Glycolysis by Pulsatile Shear Stress in Endothelial Cells

Yue Han, Ming He, Traci Marin, Hui Shen, Wei-Ting Wang, Tzong-Yi Lee, Hsiao-Chin Hong, Zong-Lai Jiang, Theodore Garland, Jr., John Y-J. Shyy, Brendan Gongol, and Shu Chien

Brendan Gongol
Email: Brendan.gongol@ucr.edu

This PDF file includes:

Supplementary Information Text

Materials and Methods

EC culture, siRNA transfection, adenoviral infection, and shear stress experiment

HUVECs obtained from Cell Applications (San Diego, CA) were cultured in M199 medium (Gibco) supplemented with 15% fetal bovine serum (FBS, Thermo Fisher), 1 ng/ml recombinant human fibroblast growth factor, 90 μg/ml heparin, 20 mM HEPES (pH 7.4), and 100 U/ml penicillin-streptomycin. For HUVEC infection, confluent cells were treated with Ad-null or Ad-KLF4 for 8 hours prior to changing the medium. Following infection, cells were recovered for 24 hours prior to harvesting or subjection to additional treatments. For siRNA knockdown, HUVECs were transfected with KLF4 siRNA at 50 nmol/L with Lipofectamine 2000 (Life Technologies). The following siRNAs were used from Qiagen: control cat #: 1027280, KLF4: cat #: SI00463239. HUVECs were plated on glass slides coated with collagen (Sigma Aldrich Cat # C7661-5MG) which were then loaded into flow channels and subjected to shear stress. Briefly, a circulating flow system was applied to impose atheroprotective pulsatile shear stress (PS, 12±4 dyn/cm^2) or atheroprone oscillatory shear stress (OS, 1±4 dyn/cm^2). The flow system was held at 37ºC with 5% CO_2.

Kinase activity assay

AMPK kinase assays were performed as previously described (18). Reactions containing 50 mM HEPES, 0.375 mM AMP, 0.375 mM ATP, 9 mM $MgCl_2$, and 2 mg GCKR with and with 11 pM AMPK were incubated at 37^oC for 1 hour. Reactions were then resolved by SDS-polyacrylamide gel electrophoresis (SDS-PAGE) prior to western blotting.

Co-immunoprecipitation and chromatin immunoprecipitation

Cell lysates harvested in FA lysis buffer (50 mM HEPES-KOH, pH 7.5, 140 mM NaCl, 1 mM EDTA, 1% Triton X-100, 0.1% sodium deoxycholate, 0.1% SDS, Halt protease inhibitors) were incubated in primary antibody bound protein A conjugated sepharose beads overnight. Beads were then washed three times with FA lysis buffer prior to immunoblotting. Following

completion of the immunoprecipitation, resulting DNA was purified with Qiagen RCP purification kit prior to qPCR analysis. Primers used for analysis are listed in Suppl Table 1.

Quantitative PCR (qPCR) and immunoblotting

RNA was purified with TRIzol reagent (Life technologies cat # 10296-028). RNA was converted to cDNA with Promega reverse transcriptase (cat # M1701) and qPCR was conducted using iQTM SYBR Green PCR supermix purchased from Bio Rad in the ABI 7500 Real-time detection system. The Δ-Δ Ct method was used to compute results. All primers used are listed in Suppl Table 1. For immunoblotting, PVDF membranes were blocked in 5% milk diluted in TBST (50 mM Tris-HCl, pH 7.4, 150 mM NaCl, 0.1% Tween 20). Membranes were then washed three times with TBST, incubated with primary antibody (Anti-KLF4 and anti-GCKR antibodies were from Cell Signaling and the anti-phosphor-GCKR S481 was generated by Genway Biotech) diluted in TBST overnight followed by secondary antibody for one hour. Following three washed with TBST, membranes were incubated with chemiluminescent Horseradish peroxidase (HRP) substrate prior to film exposure and development. For anti-phosphor-GCKR S481, we performed confirmation experiments first to ensure its specificity recognizing P-GCKR S481 (Suppl Fig. 2).

GCKR mutagenesis

Plasmid pHA-GCKR was constructed by inserting the corresponding full-length DNA fragment of GCKR into EcoRI/NotI-digested pcDNA3-HA (Invitrogen) or EcoRI/BamHI/-digested pEGFP-C1 (Clontech).

Hexokinase activity and extracellular acidification (ECAR) assays

Hexokinase activity was measured using a hexokinase assay kit (abcam cat# ab136957) according to the manufacturer's instructions. Overall glycolysis activity was measured with the glycolysis assay kit that measures extracellular acidification (abcam cat# ab197244) according to the manufacturer's instructions.

ATAC-seq

After washing two times with PBS, nuclei were isolated from ECs lysed in lysis buffer containing 10 mmol/L Tris-HCl, 10 mmol/L NaCl, 3 mmol/L MgCl2, and 0.1% NP-40. Resulting nuclei were incubated at 37^{o}C in 50 µL transposition buffer (Nextera DNA Library Preparation Kit; Illumina) and 22.5 µL H_2O for 30 minutes. DNA samples were then purified with Qiagen MinElute PCR purification kit followed by library preparation and sequencing in the IGM Genomics Core, University of California, San Diego.

Bioinformatics and statistics

All bioinformatics analyses were conducted in R and Python programming languages. Read alignments were conducted with hisat2 with support from the systempipeR Bioconductor package and fold changes and statistics were calculated with EdgeR. ATACseq or H3K27 CHIP-seq data was analyzed with the systempipeR bioconductor package. Reads were aligned with Bowtie2 and relative enrichment was computed with MACS2. Phosphorylation consensus sequences were identified using pattern matching functions housed in the stringr R package. All statistical analyses were performed with GraphPad Prism 7 software or R. The Student t test or Mann-Whitney U test were used for comparisons between 2 groups. Data were expressed as mean ± SEM and $p<0.05$ was considered to be statistically significant.

A

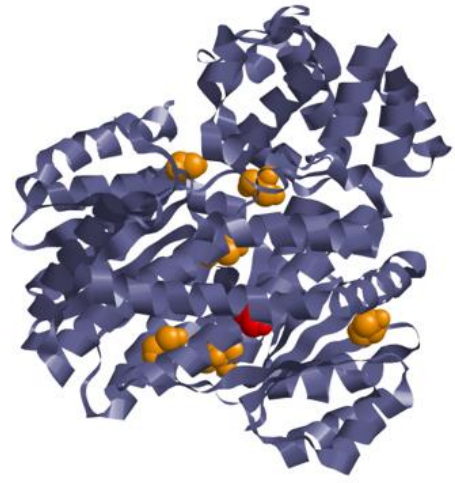

B

Common_marmoset_monkey	414	NFIQKFQRELSTKWVLNTVST	434
Mouse	471	SYVQKFQRELSTKWVLNTVST	491
Rat	471	TYVQKFQRELSTKWVLNTVST	491
Guinea	471	NFVQKFQRELSTKWVLNTVST	491
Green	471	NFVQKFQRELSTKWVLNTVST	491
Gorilla	471	NFIQKFQRELSTKWVLNTVST	491
Human	471	NFIQKFQRELSTKWVLNTVST	491
Giant	471	NFIQKFQHELSTKWVLNTVST	491
Horse	471	NFIQKFQHELSTKWVLNTVST	491
AMPK consensus sequence		XXXXβφβXXXSXXXβXXXXXX	

Fig. S1. The prediction of AMPK phosphorylation sites of GCKR and GCKR phosphorylation site conservation: (A) Crystal structure of GCKR (PDBID: 4BB9) highlighted with predicted AMPK phosphorylation sites (yellow). S481 is highlighted in red. (B) GCKR sequence pile up indicating conservation of the S481 AMPK phosphorylation site and conformity to the AMPK consensus sequence.

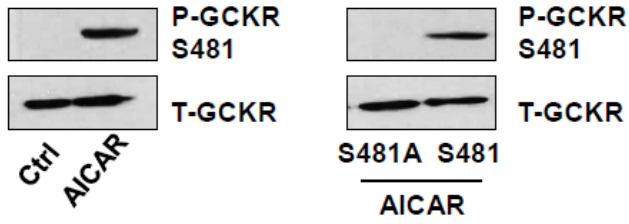

Fig. S2. The specificity of anti-phosphor-GCKR S481. Left panel: The phosphorylation level of GCKR S481 was increased in HUVECs treated with AICAR but not in untreated Ctrl cells. Right Panel: AICAR increased the phosphorylation level of GCKR S481 in HUVECs transfected with plasmids expressing native GCKR compared to those expressing S481A GCKR.

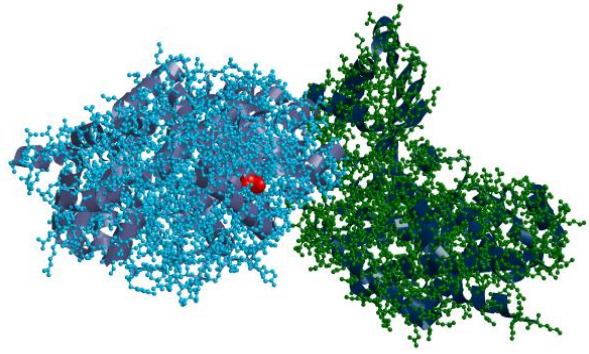

Fig. S3. Crystal structure of GCKR:HK complex (PDBID: 4LC9) highlighted with S481 on GCKR in red. GCKR is colored blue and HK is green.

Table S1. Primer sequences

Gene Name	Direction	Sequence	Species	Type	source
ALDOA	Forward	GCCCGTTATGCCAGTATCTG	Human	mRNA	
ALDOA	Reverse	CACTCAGAGCCTTGTAGACAG	Human	mRNA	
ENO3	Forward	TGGGAAGGATGCCACCAATGTG	Human	mRNA	origene CAT#: HP205737
ENO3	Reverse	GCGATAGAACTCAGATGCTGCC	Human	mRNA	origene CAT#: HP205737
GAPDH	Forward	ACATCGCTCAGACACCATG	Human	mRNA	
GAPDH	Reverse	ATGACAAGCTTCCCGTTCTC	Human	mRNA	
GCKR	Forward	AGCGAATCCATTCTGACCAC	Human	mRNA	
GCKR	Reverse	GGTGTAAAGAGGTTTCTGTCCC	Human	mRNA	
GPI1	Forward	CTGGTAGACGGCAAGGATGTGA	Human	mRNA	origene CAT#: HP200160
GPI1	Reverse	TCCGTGATGGTCTTGCCTGTGT	Human	mRNA	origene CAT#: HP200160
HK1	Forward	GTCTGAATGTGACTGTGGGAG	Human	mRNA	
HK1	Reverse	TCTGGTGCATGATTCTGGAG	Human	mRNA	
LDHA	Forward	CGTCAGCAAGAGGGAGAAAG	Human	mRNA	
LDHA	Reverse	GCCACGTAGGTCAAGATATCC	Human	mRNA	
PFKM	Forward	GGAAAACCAATCACCTCAGAAG	Human	mRNA	
PFKM	Reverse	GCTTCCACACCCATCCTG	Human	mRNA	
PGAM1	Forward	GCTCTGCCCTTCTGGAATGAAG	Human	mRNA	origene CAT#: HP206283
PGAM1	Reverse	ATACCAGTCGGCAGGTTCAGCT	Human	mRNA	origene CAT#: HP206283
PGK1	Forward	GATTACCTTGCCTGTTGACTTTG	Human	mRNA	
PGK1	Reverse	TGACAGCCTCAGCATACTTC	Human	mRNA	
PKM	Forward	ATTCCTGCTACAGTCTCCAAC	Human	mRNA	
PKM	Reverse	CAATGATAAACACCCGACGC	Human	mRNA	
TPI1	Forward	GGAAACTGGAAGATGAACGGG	Human	mRNA	
TPI1	Reverse	AATCTTGGGATCTAGCTTCTGC	Human	mRNA	
ALDOA	Forward	TTCAGGCTCTTTCCCATCAC	Mouse	mRNA	
ALDOA	Reverse	TGGAAGGGATGGCAGATTTAG	Mouse	mRNA	
ENO3	Forward	ATCCTGGAGAACAATGAGGC	Mouse	mRNA	
ENO3	Reverse	TCCAGATCATACTTGCCGTTG	Mouse	mRNA	
GAPDH	Forward	AGGCCGGTGCTGAGTATGTC	Mouse	mRNA	
GAPDH	Reverse	TGCCTGCTTCACCACCTTCT	Mouse	mRNA	
GCKR	Forward	GGGAGCTACGTTCAGAAGTTC	Mouse	mRNA	
GCKR	Reverse	AGCGGTTGAGGGAAATGTATC	Mouse	mRNA	
GPI1	Forward	CCATCAAGGTGGACGGCAAAGA	Mouse	mRNA	origene CAT#:

					MP205497
GPI1	Reverse	CCGTGATGGATTTGCCAGTGTAC	Mouse	mRNA	origene CAT#: MP205497
HK	Forward	CGTGCCGACAATCCAAAATAG	Mouse	mRNA	
HK	Reverse	AATGTTAGCGTCATAGTCCCC	Mouse	mRNA	
LDHA	Forward	GCTCCCCAGAACAAGATTACAG	Mouse	mRNA	
LDHA	Reverse	TCGCCCTTGAGTTTGTCTTC	Mouse	mRNA	
PFKM	Forward	ACCGAATCCCCAAAGAACAG	Mouse	mRNA	
PFKM	Reverse	TTCTCCAGACCGTTTCCTTG	Mouse	mRNA	
PGAM1	Forward	CCCCTTCTACAGCAACATCAGC	Mouse	mRNA	origene CAT#: MP210922
PGAM1	Reverse	GCTCTGGCAATAGTGTCCTTCAG	Mouse	mRNA	origene CAT#: MP210922
PGK1	Forward	AACCTCCGCTTTCATGTAGAG	Mouse	mRNA	
PGK1	Reverse	GACATCTCCTAGTTTGGACAGTG	Mouse	mRNA	
PKM	Forward	CAGAGAAGGTCTTCCTGGCTCA	Mouse	mRNA	origene CAT#: MP212273
PKM	Reverse	GCCACATCACTGCCTTCAGCAC	Mouse	mRNA	origene CAT#: MP212273
TPI1	Forward	TCGAGCAAACCAAGGTCATC	Mouse	mRNA	
TPI1	Reverse	GCTTCTCGTGTACTTCCTGTG	Mouse	mRNA	
GCKR	Forward	TGACCAGAGGGGTTTGTGTG	Human	ChIP	
GCKR	Reverse	AGAGGTGAGCAGAAACCAGC	Human	ChIP	
GCKR	Forward	GTGTCTCTAGTTGTCAGGGTATG	Mouse	ChIP	
GCKR	Reverse	AATCCTTCCACATCACAAAACAG	Mouse	ChIP	

References

1. A. Doddaballapur, K.M. Michalik, Y. Manavski, T. Lucas, R.H. Houtkooper, X. You, W. Chen, A.M. Zeiher, M. Potente, S. Dimmeler, R.A. Boon, Laminar shear stress inhibits endothelial cell metabolism via KLF2-mediated repression of PFKFB3. *Arterioscler. Thromb. Vasc. Biol.* 35, 137-145 (2015).
2. J. Wang, S. Zhang, Fluid shear stress modulates endothelial inflammation by targeting LIMS2. *Exp. Biol. Med.* 245, 1656-1663 (2020).
3. S. Chien, Effects of disturbed flow on endothelial cells. *Ann. Biomed. Eng.* 36, 554-62 (2008).
4. K. Heo, K. Fujiwara, J. Abe, Disturbed-flow-mediated vascular reactive oxygen species induce endothelial dysfunction. *Circ. J.* 75, 2722-2730 (2011).
5. P.F. Davies, A. Remuzzi, E.J. Gordon, C.F. Dewey Jr., M.A. Gimbrone Jr., Turbulent fluid shear stress induces vascular endothelial cell turnover in vitro. *Proc. Natl. Acad. Sci. U.S.A.* 83, 2114-2117 (1986).
6. J. Chiu, S. Chien, Effects of disturbed flow on vascular endothelium: pathophysiological basis and clinical perspectives. *Physiol. Rev.* 91, 327-387 (2011).
7. K. Theodorou, R.A. Boon, Endothelial cell metabolism in atherosclerosis. *Front. Cell. Dev. Biol.* 6, 82 (2018).
8. K. Rohlenova, K.D. Veys, I. Miranda-Santos, K.D. Bock, P. Carmeliet, Endothelial cell metabolism in health and disease. *Trends. Cell. Biol.* 28, 224-236 (2018).
9. G. Eelen, P. Zeeuw, M. Simons, P. Carmeliet, Endothelial cell metabolism in normal and diseased vasculature. *Circ. Res.* 116, 1231-1244 (2015).
10. K.D. Bock, M. Georgiadou, P. Carmeliet, Role of endothelial cell metabolism in vessel sprouting. *Cell. Metab.* 18, 634-647 (2013).
11. D. Wu, R.T. Huang, R.B. Hamanaka, M. Krause, M.J. Oh, C.H. Kuo, R. Nigdelioglu, A.Y. Meliton, L. Witt, G. Dai, M. Civelek, N.R. Prabhakar, Y. Fang, G.M. Mutlu, HIF-1α is required for disturbed flow-induced metabolic reprogramming in human and porcine vascular endothelium. *Elife.* 6, e25217 (2017).
12. S. Feng, N. Bowden, M. Fragiadaki, C. Souilhol, S. Hsiao, M. Mahmoud, S. Allen, D. Pirri, B.T. Ayllon, S. Akhtar, R. Thompson, H. Jo, C. Weber, V. Ridger, A. Schober, P.C. Evans, Mechanical Activation of Hypoxia-Inducible Factor 1α Drives Endothelial Dysfunction at Atheroprone Sites. *Arterioscler. Thromb. Vasc. Biol*. 37, 2087-2101 (2017).
13. A. Young, W. Wu, W. Sun, H.B. Larman, N. Wang, Y. Li, J.Y. Shyy, S. Chien, G. García-Cardeña, Flow activation of AMP-activated protein kinase in vascular endothelium leads to Krüppel-like factor 2 expression. *Arterioscler. Thromb. Vasc. Biol.* 29, 1902-1908 (2009).
14. Y. Fan, H. Lu, W. Liang, W. Hu, J. Zhang, E. Chen, Krüppel-like factors and vascular wall homeostasis. *J. Mol. Cell. Biol.* 9, 352-363 (2017).
15. G. Zhou, A. Hamik, L. Nayak, H. Tian, H. Shi, Y. Lu, N. Sharma, X. Liao, A. Hale, L. Boerboom, R.E. Feaver, H. Gao, A. Desai, A. Schmaier, S.L. Gerson, Y. Wang, G.B. Atkins, B.R. Blackman, D.I. Simon, M.K. Jain, Endothelial Kruppel-like factor 4 protects against atherothrombosis in mice. *J. Clin. Invest.* 122, 4727-4731. (2012).
16. M. He, T.S. Huang, S. Li, H.C. Hong, Z. Chen, M. Martin, X. Zhou, H.Y. Huang, S.H. Su, J. Zhang, W.T. Wang, J. Kang, H.D. Huang, J. Zhang, S. Chien, J.Y. Shyy, Atheroprotective flow upregulates ITPR3 (Inositol 1,4,5-Trisphosphate Receptor 3) in vascular endothelium via KLF4 (Krüppel-Like Factor 4)-mediated histone modifications. *Arterioscler. Thromb. Vasc. Biol.* 39, 902-914 (2019).
17. T.L. Marin, B. Gongol, F. Zhang, M. Martin, D.A. Johnson, H. Xiao, Y. Wang, S. Subramaniam, S. Chien, J.Y. Shyy, AMPK promotes mitochondrial biogenesis and function by phosphorylating the epigenetic factors DNMT1, RBBP7, and HAT1. *Sci. Signal.* 10, eaaf7478 (2017).
18. T.L. Marin, B. Gongol, M. Martin, S.J. King, L. Smith, D.A. Johnson, S. Subramaniam, S. Chien, J.Y. Shyy, Identification of AMP-activated protein kinase targets by a consensus sequence search of the proteome. *B.M.C. Syst. Biol.* 9, 13 (2015).

19. B. Thors, H. Halldórsson, G. Thorgeirsson, eNOS activation mediated by AMPK after stimulation of endothelial cells with histamine or thrombin is dependent on LKB1. *Biochim. Biophy.s Acta*. 1813, 322-331 (2011).
20. J. Zhang, J. Dong, M. Martin, M. He, B. Gongol, T.L. Marin, L. Chen, X. Shi, Y. Yin, F. Shang, Y. Wu, H. Huang, J. Zhang, Y. Zhang, J. Kang, E.A. Moya, H. Huang, F.J. Powell, Z. Chen, P.A. Thistlethwaite, Z. Yuan, J. Shyy, AMP-activated Protein Kinase Phosphorylation of Angiotensin-Converting Enzyme 2 in Endothelium Mitigates Pulmonary Hypertension. *Am. J. Respir. Crit. Care. Med.* 15, 509-520 (2018).
21. A. Raimondo, M.G. Rees, A.L. Gloyn, Glucokinase regulatory protein: complexity at the crossroads of triglyceride and glucose metabolism. *Curr. Opin. Lipidol.* 26, 88-95 (2015).
22. M. Salgado, P. Ordenes, M. Villagra, E. Uribe, M.L.A. García-Robles, E. Tarifeño-Saldivia, When a little bit more makes the difference: expression levels of GKRP determines the subcellular localization of GK in tanycytes. *Front. Neurosci.* 13, 275 (2019).
23. B. Guigas, L. Bertrand, N. Taleux, M. Foretz, N. Wiernsperger, D. Vertommen, F. Andreelli, B. Viollet, L. Hue, 5-Aminoimidazole-4-carboxamide-1-beta-D-ribofuranoside and metformin inhibit hepatic glucose phosphorylation by an AMP-activated protein kinase-independent effect on glucokinase translocation. *Diabetes.* 55, 865-874 (2006).
24. N.E. Ajami, S. Gupta, M.R. Maurya, P. Nguyen, J.Y. Li, J.Y. Shyy, Z. Chen, S. Chien, S. Subramaniam, Systems biology analysis of longitudinal functional response of endothelial cells to shear stress. *Proc. Natl. Acad. Sci.* 114, 10990-10995 (2017).
25. D.R. Zerbino, P. Achuthan, W. Akanni, M.R. Amode, D. Barrell, J. Bhai, K. Billis, C. Cummins, A. Gall, C.G. Girón, L. Gil, L. Gordon, L. Haggerty, E. Haskell, T. Hourlier, O.G. Izuogu, S.H. Janacek, T. Juettemann, J.K. To, M.R. Laird, I. Lavidas, Z. Liu, J.E. Loveland, T. Maurel, W. McLaren, B. Moore, J. Mudge, D.N. Murphy, V. Newman, M. Nuhn, D. Ogeh, C.K. Ong, A. Parker, M. Patricio, H.S. Riat, H. Schuilenburg, D. Sheppard, H. Sparrow, K. Taylor, A. Thormann, A. Vullo, B. Walts, A. Zadissa, A. Frankish, S.E. Hunt, M. Kostadima, N. Langridge, F.J. Martin, M. Muffato, E. Perry, M. Ruffier, D.M. Staines, S.J. Trevanion, B.L. Aken, F. Cunningham, A. Yates, P. Flicek, Ensembl 2018. *Nucleic. Acids. Res.* 46, D754-D761 (2018).
26. L. Agius, Hormonal and metabolite regulation of hepatic glucokinase. *Annu. Rev. Nutr.* 36, 389-415 (2016).
27. A. Šmerc, E. Sodja, M. Legiša, Posttranslational modification of 6-phosphofructo-1-kinase as an important feature of cancer metabolism. *PLoS. One.* 6, e19645 (2011).
28. Y. Zhang, T.S. Lee, E.M. Kolb, K. Sun, X. Lu, F.M. Sladek, G.S. Kassab, T. Garland Jr., J.Y. Shyy, AMP-activated protein kinase is involved in endothelial NO synthase activation in response to shear stress. *Arterioscler. Thromb. Vasc. Biol.* 26, 1281-1287 (2006).
29. L.M. Vaanholt, I. Jonas, M. Doornbos, K.A. Schubert, C. Nyakas, T. Garland, G.H. Visser, G. Dijk, Metabolic and behavioral responses to high-fat feeding in mice selectively bred for high wheel-running activity. *Int. J. Obes.* 32, 1566-1575 (2008).
30. K.S. Zaret, Pioneer Transcription Factors Initiating Gene Network Changes. *Annu. Rev. Genet.* 54, 367-385 (2020).
31. A. Moosavi, A.M. Ardekani, Role of Epigenetics in Biology and Human Diseases. *Iran. Biomed. J.* 20, 246-258 (2016).
32. J. Grimsby, J.W. Coffey, M.T. Dvorozniak, J. Magram, G. Li, F.M. Matschinsky, C. Shiota, S. Kaur, M.A. Magnuson, J.F. Grippo, Characterization of glucokinase regulatory protein-deficient mice. *J. Biol. Chem.* 275, 7826-7831 (2000).
33. B. Viollet, F. Andreelli, S.B. Jørgensen, C. Perrin, D. Flamez, J. Mu, J.F.P. Wojtaszewski, F.C. Schuit, M. Birnbaum, E. Richter, R. Burcelin, S. Vaulont, Physiological role of AMP-activated protein kinase (AMPK): insights from knockout mouse models. *Biochem. Soc. Trans.* 31, 216-219 (2003).
34. J. Park, T. Kim, S. Jo, M. Kim, Y. Ahn, Acetylation of glucokinase regulatory protein decreases glucose metabolism by suppressing glucokinase activity. *Sci. Rep*. 5, 17395 (2015).
35. Q. Yang, J. Xu, Q. Ma, Z. Liu, V. Sudhahar, Y. Cao, L. Wang, X. Zeng, Y. Zhou, M. Zhang, Y. Xu, Y. Wang, N.L. Weintraub, C. Zhang, T. Fukai, C. Wu, L. Huang, Z. Han, T.

Wang, D.J. Fulton, M. Hong, Y. Huo, PRKAA1/AMPKα1-driven glycolysis in endothelial cells exposed to disturbed flow protects against atherosclerosis. *Nat. Commun.* 9, 4667 (2018).
36. G. Soto-Heredero, M.M. Gómez de Las Heras, E. Gabandé-Rodríguez, J. Oller, M. Mittelbrunn, Glycolysis - a key player in the inflammatory response. *FEBS. J.* 287, 3350-3369 (2020).
37. C.M. Grant, Metabolic reconfiguration is a regulated response to oxidative stress. *J. Biol*. 7, 1 (2008).